Received: 2 December 2021 | Revised: 4 March 2022 | Accepted: 21 March 2022

DOI: 10.1002/nbm.4734

REVIEW ARTICLE

NMR IN BIOMEDICINE WILEY

Amide proton transfer imaging in stroke

Hye-Young Heo[1,2] | Yee Kai Tee[3] | George Harston[4] | Richard Leigh[5] | Michael A. Chappell[6,7,8]

[1]Division of MR Research, Department of Radiology, Johns Hopkins University School of Medicine, Baltimore, Maryland, USA

[2]F.M. Kirby Research Center for Functional Brain Imaging, Kennedy Krieger Institute, Baltimore, Maryland, USA

[3]Lee Kong Chian Faculty of Engineering and Science, University Tunku Abdul Rahman, Malaysia

[4]Acute Stroke Programme, Oxford University Hospitals NHS Foundation Trust, Oxford, UK

[5]Department of Neurology, Johns Hopkins University School of Medicine, Baltimore, Maryland, USA

[6]Radiological Sciences, Mental Health and Clinical Neurosciences, School of Medicine, University of Nottingham, Nottingham, UK

[7]Nottingham Biomedical Research Centre, Queen's Medical Centre, University of Nottingham, Nottingham, UK

[8]Sir Peter Mansfield Imaging Centre, School of Medicine, University of Nottingham, Nottingham, UK

Correspondence
Hye-Young Heo PhD, Division of MR Research, Department of Radiology, Johns Hopkins University School of Medicine, 600 N. Wolfe Street, Park 336, Baltimore, MD 21287, USA.
Email: hheo1@jhmi.edu

Michael Chappell PhD, University of Nottingham, Beacon Hub Offices, A floor, Medical School, QMC, Nottingham NG7 2UH, UK.
Email: michael.chappell@nottingham.ac.uk

Funding information
American Heart Association, Grant/Award Number: 20IPA35310888, HYH; National Institutes of Health, Grant/Award Numbers: P41EB0311771, HYH, R01NS112242, HYH; Ministry of Higher Education Malaysia under the Fundamental Research Grant Scheme, Grant/Award Number: FRGS/1/2021/ICT02/UTAR/02/2, YKT; UTAR Research Fund, Grant/Award Number: IPSR/RMC/UTARRF/2020-C1/T02, YKT; National Cancer Council Malaysia, YKT

Amide proton transfer (APT) imaging, a variant of chemical exchange saturation transfer MRI, has shown promise in detecting ischemic tissue acidosis following impaired aerobic metabolism in animal models and in human stroke patients due to the sensitivity of the amide proton exchange rate to changes in pH within the physiological range. Recent studies have demonstrated the possibility of using APT-MRI to detect acidosis of the ischemic penumbra, enabling the assessment of stroke severity and risk of progression, monitoring of treatment progress, and prognostication of clinical outcome. This paper reviews current APT imaging methods actively used in ischemic stroke research and explores the clinical aspects of ischemic stroke and future applications for these methods.

KEYWORDS
APT, CEST, ischemic penumbra, pH imaging, stroke

Abbreviations: ADC, apparent diffusion coefficient; APT, amide proton transfer; APTw, APT weighted; CBF, cerebral blood flow; CEST, chemical exchange saturation transfer; CT, computed tomography; DWI, diffusion-weighted imaging; ED, emergency department; EMR, extrapolated semisolid magnetization transfer reference; MCAO, middle cerebral artery occlusion; mRS, modified Rankin scale; MTR, magnetization transfer ratio; NIHSS, National Institutes of Health Stroke Scale; NOE, nuclear Overhauser enhancement; PET, positron emission tomography; PWI, perfusion-weighted imaging.

1 | INTRODUCTION

Ischemic stroke occurs when there is hypoperfusion of an area of the brain, which is typically caused by a vascular occlusion. Distal to the occlusion, the affected vascular territory is often characterized by a smaller ischemic core that suffers infarction, which is surrounded by a larger area of marginally perfused tissue, typically referred to as the ischemic penumbra. Different types of penumbra have been defined over the years. Classically, neurons within the penumbra are unable to maintain a resting potential and become dysfunctional, but are not yet irreversibly damaged, for example in cases where the blood flow supplied by collateral arteries is adequate to prevent cellular membrane breakdown and mitochondrial death.[1–4] However, unless rapidly reversed, ongoing ischemia may result in metabolic derangements and neuronal death. Ultimately, the infarct core may grow and progressively replace the ischemic penumbra. Thus, the major goal of intervention in acute ischemic stroke is to salvage the ischemic penumbra.[1,5–8] Although a number of sensitive imaging methods have been developed to evaluate the physiological state of brain tissue, the current standard of care in most hospitals is time dependent, which limits imaging to a computed tomography (CT) scan to exclude hemorrhage. Unfortunately, this approach ignores the variability that each subject shows and rejects the possibility of treatment for about 90% of stroke patients whose clinical course does not fit a fixed time window.[9–12] This under-use of imaging methods due to time constraints is unfortunate because the identification of a true ischemic penumbra could lead to more rational treatment decisions, as well as active successful outcomes outside conventional time windows. The rate of change in the size of the ischemic penumbra varies from patient to patient, depending on collateral circulation. Two randomized "late window" mechanical thrombectomy trials showed that patients with salvageable tissues had less disability and were more likely to be functionally independent at 90 days after initiation of endovascular thrombectomy between 6 and 16 h or up to 24 h after the patient was last known to be well.[13–15] Similarly, a late time window thrombolysis trial using perfusion imaging showed an opportunity to personalize treatment selection and extend the time window for treatments of a subset of patients.[16] These trials suggest that, as long as patients are robustly phenotyped for the presence of an ischemic penumbra, treatment decisions can be personalized, rather than being based on arbitrary time windows, expanding the treatable population. This situation strongly emphasizes the urgent need for improved and accessible imaging techniques to readily define the salvageable penumbra from the irreversibly damaged infarct core at the level of the individual.

Positron emission tomography (PET) first demonstrated the ability to image the ischemic penumbra in vivo, defined by quantitative PET parameters, such as cerebral blood flow (CBF), and is considered the "gold standard" in the early evaluation of acute stroke pathophysiology.[2,17–19] However, the use of quantitative PET is unfortunately limited by a lack of availability in emergency settings, the need for arterial catheterization, the administration of radioactive tracers, and long scan times, making it impractical in the hyperacute stroke setting with a time-limited opportunity for intervention. Clinically, CT and CT angiography (CTA) are the primary imaging modalities for the emergency assessment of suspected acute stroke, mainly to identify vascular occlusion, exclude hemorrhagic stroke prior to thrombolytic treatment, assess collateral circulation in the territory of the occluded artery, and assess irreversibly damaged tissue during very early ischemia, albeit in a less detailed way than is possible using PET or MRI.[20–22] While such approaches have been partially successful due to a heavy reliance on the speed of treatment, they currently do not provide information about changes in physiological tissue status related to pH, metabolism, and acute cell depolarization, all of which may provide more sensitive and specific markers of tissue viability. Although CT perfusion (CTP) is promising for the identification of a perfusion-based ischemic penumbra, measures of perfusion parameters are not directly translatable to events at the cellular level, and thus can provide only an indirect estimate of whether tissue is viable.

During the past few decades, MRI techniques have gained a small role in the acute management of stroke.[23] Typically, diffusion-weighted imaging (DWI) is used to visualize early membrane depolarization through changes in the local diffusion properties of water in the ischemic lesion, while perfusion-weighted imaging (PWI) provides quantitative information about abnormal CBF or volume. The DWI–PWI spatial mismatch has been used to identify the presence of a flow-based ischemic penumbra and, over the past two decades or more, been tested as a selection marker for thrombolysis.[5,24,25] Unfortunately, the use of the DWI/PWI mismatch concept has proven to be limited in routine clinical application due to variable sensitivity, specificity, and high false-negative rates.[26–29] One of the main issues is that the mismatch area often overestimates the size of the ischemic penumbra and includes regions of benign oligemia. This is particularly true in the setting of chronic vascular occlusions that may appear as penumbra with DWI/PWI, but are stable at the physiologic level. Preclinical animal studies indicate that a more appropriate ischemic penumbra would be the region in which oxidative metabolism is impaired, but no diffusion changes have occurred,[30,31] and reviews by leading experts have suggested that this should be the required criterion.[2,18,19,30] Attempts to better specify such a true penumbra through the addition of mean transit time cutoff criteria on PWI are promising, but not yet conclusive.[32–36] Alternatively, previous clinical studies (e.g., Wake-Up Stroke trial) demonstrated that DWI/fluid-attenuated inversion recovery (FLAIR) mismatch can be used as a surrogate marker to identify patients eligible for intravenous thrombolysis.[37,38] However, the concept of mismatch of DWI–FLAIR is thought to indirectly estimate the onset time in acute ischemic stroke patients, not specifically penumbra identification and quantification.

Previous papers have reviewed the basic chemical exchange saturation transfer (CEST) or amide proton transfer (APT) principles, recent technical developments, and current and emerging clinical applications including stroke imaging.[39–42] Herein, we highlight current APT imaging technologies actively used in ischemic stroke research, and important limitations and challenges of current APT-based penumbra imaging, and end with possible solutions and future directions.

2 | BRAIN TISSUE ACIDOSIS IN ISCHEMIA

A simplified overview of the approximate CBF thresholds[2,18,19,30] and their relationship to MR parameters[41] is shown in Figure 1. The original concept of the ischemic penumbra was defined by the thresholds of (1) electrical failure, encompassing functionally impaired but structurally intact neurons, which corresponds to an approximate CBF range of 8–18 mL/100 g/min, and (2) membrane failure, encompassing functionally and structurally impaired neurons (likely irreversible damage, i.e., infarction), which corresponds to a CBF of about 8 mL/100 g/min or less. The intermediate zone (yellow-shaded area in Figure 1A) is referred to as the classic ischemic penumbra, a region with neuronal dysfunction but no cellular energy failure. Eventually, below a CBF threshold of about 8 mL/100 g/min, anoxic depolarization occurs, leading to intracellular accumulation of sodium, calcium, and water (cytotoxic edema). Although reversible changes in water shifts have been measured after membrane failure,[43,44] as confirmed by recent clinical imaging results, anoxic depolarization mostly leads to infarction, except in the case of very short ischemic durations. Thus, further investigation of the DWI-based core with physiologic imaging may better define the inner edge of the ischemic penumbra as well.

The current understanding of a true ischemic penumbra is based on the concept that tissue can be impaired because of a deficit in oxidative metabolism, but can be still viable. Such tissue surrounds and is contiguous with an area of irreversible cerebral infarction.[1,2] Acute cerebral ischemia causes a shift to anaerobic glycolysis, resulting in the accumulation of lactic acid and a concomitant decrease in intracellular pH.[45] Therefore, tissue acidosis is the earliest sign that tissue is at risk. If ischemic acidosis can be imaged, salvageable tissue at risk of infarction could be visualized by subtracting the extent of the diffusion deficit (cellular depolarization) from the pH deficit extent (anaerobic metabolism).

3 | APT PRECLINICAL RESEARCH

Based on the CEST-MRI principle, it is possible to detect the MRI signal of tissue mobile proteins and peptides, such as those in the cytoplasm, through chemical exchange between exchangeable amide protons (–NH) in the protein peptide bonds and tissue water.[39,46–48] While the effect of millimolar concentrations of amide protons on the water resonance (~110 M protons) is not detectable, the cumulative effect of repeated saturation and chemical exchange, in which saturated amide protons move to water and are replaced by unsaturated water protons from the large water pool, which are then saturated, allows sensitivity enhancements of 100–1000-fold. Thus, specific molecular information can be obtained indirectly through the bulk water signal.

Amide protons in the backbone of solute proteins resonate around +3.5 ppm downfield of the water signal, and interact with water protons through chemical exchange.[49] The exchange rate of these protons is highly pH dependent because their exchange rate is base catalyzed in the physiological pH range, and typically decreases tenfold per unit of pH drop.[50] Therefore, the APT signal is reduced in the ischemic area since intracellular pH is lower in the ischemic lesion than in normal brain tissue. Typically, pH-sensitive APT effects can be detected by acquiring a so-called

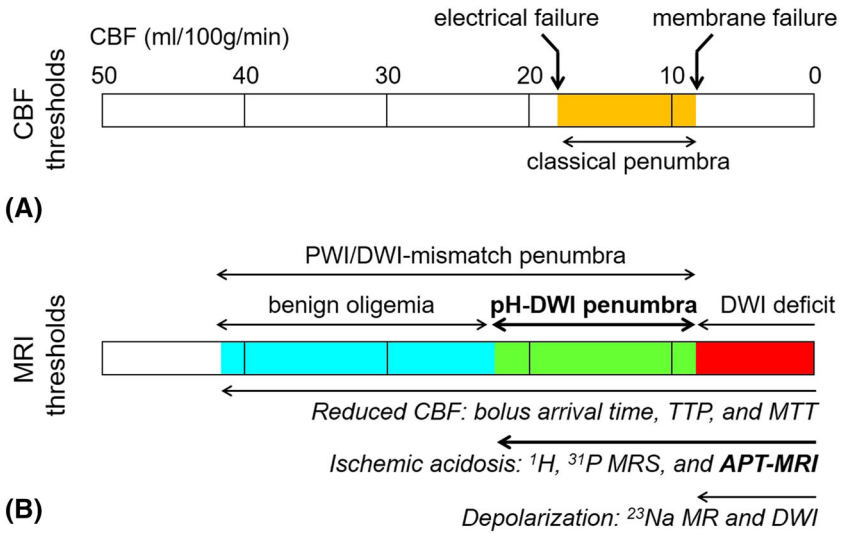

FIGURE 1 Simplified depiction of the relationship between CBF-based ischemic neurological (A) and MRI parameter (B) thresholds. Thresholds are approximate (PET-based normal gray matter CBF ~50 mL/100 g/min) and might shift to a higher CBF with a longer ischemic duration. The metabolic penumbra is indicated by yellow shading. At the bottom, zones of perfusion–DWI and pH–DWI mismatch are shown, with the difference being benign oligemia. (Reproduced, in part, with permission from Leigh et al. *J Cereb Blood Flow Metab*. 2017;38:1500-1516)

Z-spectrum, in which the ratio of water signal intensity with saturation (S_{sat}) and without saturation (S_0) is plotted as a function of saturation frequency. The APT signal intensity at 3.5 ppm from water is significantly decreased after global ischemia,[46] as shown in Figure 2. Notably, the reduced APT effect can be clearly seen in the magnetization transfer ratio (MTR = 1 − S_{sat}/S_0) spectrum, as shown in rat middle cerebral artery occlusion (MCAO) models 2 h after occlusion. The most commonly used metric with which to quantify the APT effect is defined as

$$\mathrm{MTR_{asym}}(3.5\,\mathrm{ppm}) = \mathrm{MTR}(+3.5\,\mathrm{ppm}) - \mathrm{MTR}(-3.5\,\mathrm{ppm}). \quad (1)$$

This asymmetry measure corrects for the influence of direct water saturation and other symmetric components not associated with the APT effect. Reduced $\mathrm{MTR_{asym}}$(3.5 ppm) (red arrow in Figure 2D) is attributable to a pH reduction, which causes a slower exchange. Although these APT effects are small (a few percent on the water signal), they correspond to a detection sensitivity of molar concentration. The $\mathrm{MTR_{asym}}$ at 3.5 ppm has multiple contributions:

$$\mathrm{MTR_{asym}}(3.5\,\mathrm{ppm}) = \mathrm{APTR} + \mathrm{MTR'_{asym}}(3.5\,\mathrm{ppm}) \quad (2)$$

$$\mathrm{APTR} = k_{sw}\left(\frac{[\text{amide proton}]}{[\text{water proton}]}\right)T_1\left(1 - e^{-t_{sat}/T_1}\right) \quad (3)$$

where APTR is the proton transfer ratio associated with amide protons, and an additional term, $\mathrm{MTR'_{asym}}$(3.5 ppm), accounts for asymmetric effects on the MTR spectrum not associated with APT. These effects can include intramolecular and intermolecular nuclear Overhauser enhancement (NOE) effects of aliphatic protons of mobile cellular macromolecules in tissue, including semisolid MT asymmetry. Due to these contributions, APT signals quantified by the MTR asymmetry analysis are called APT-weighted (APTw) signals.[40] Equation 3 is based on the simplified assumption of a two-pool exchange model (free bulk water and amide proton pools), in which APTR is proportional to the ratio of amide proton and water proton concentration (square brackets, [.]), and the exchange rate (k_{sw}) from the amide proton pool to the water proton pool, which is related to tissue pH. Zhou et al. derived the calibration curve of pH using the equation, $\mathrm{APTR} = 5.73 \times 10^{\mathrm{pH}-9.4}$, by comparing the in vivo and postmortem $\mathrm{MTR_{asym}}$(3.5 ppm) signals and using ^{31}P MRS for intracellular pH assessment.[46] With the calibration formula, an absolute pH map could be generated, as shown in Figure 2A, which correctly outlined the ischemic area in the caudate nucleus, a region commonly affected by infarction following MCAO, where ischemia was confirmed by histology acquired 8 h later (Figure 2B).[46] However, the APTR–pH equation was

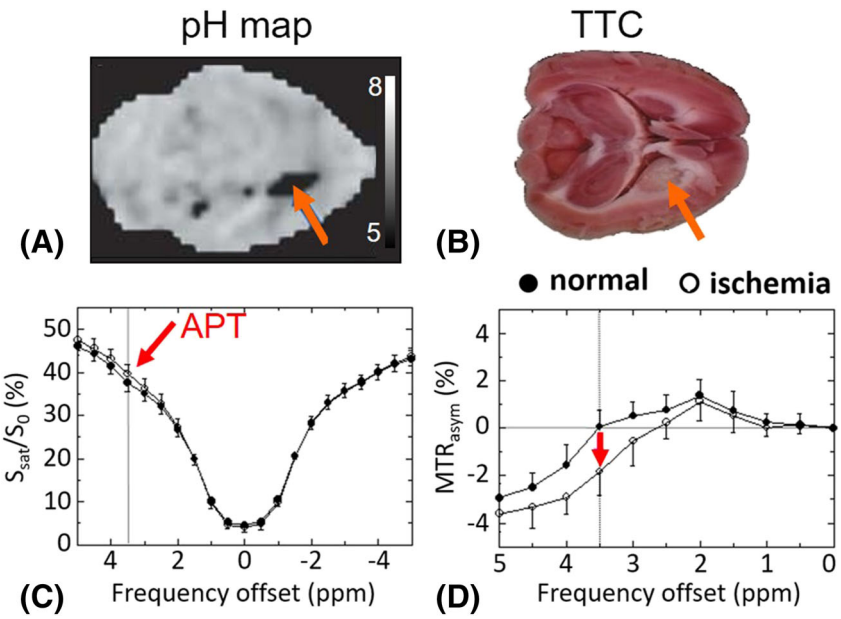

FIGURE 2 (A), A pH map of a rat MCAO model 2 h after occlusion. The average ischemic pH was 6.52 ± 0.32. (B), Triphenyl tetrazolium chloride (TTC) histology image. C, D, *Z*-spectrum (C) and MTR asymmetry spectrum (D) of the rat brain ($n = 7$). The *Z*-spectrum is a measurement of normalized water saturation (S_{sat}/S_0) as a function of RF saturation frequency. MTR = 1 − S_{sat}/S_0 asymmetric analysis is used to measure the APT signal by subtracting the MTR at −3.5 ppm, with respect to water, from that at +3.5 ppm. (Reproduced, in part, with permission from Zhou et al. *Nat Med*. 2003;9:1085-1090)

derived with several simplified assumptions, for example, negligible changes in the amide proton content, water content, water relaxation time, and the effect of temperature on the exchange rate.

Following the initial study, many APT-based pH imaging studies have demonstrated the possibility of using APT-MRI to detect an acidosis-based ischemic penumbra in rat models of permanent MCAO. Importantly, Sun et al.[51] showed that a pH deficit based on APTw MRI in the first 3.5 h correctly predicted the infarct 24 h later, as shown in Figure 3. Although two rats (Figure 3C) showed a different degree of mismatch between diffusion, pH, and perfusion deficits, only pH deficits predicted well the evolution of infarction. However, the diffusion deficit underestimated the final lesion and the perfusion deficit overestimated it. Interestingly, several animals showed negligible apparent diffusion coefficient (ADC) effects in the hyperacute state, despite the presence of perfusion and pH effects, suggesting that pH changes can occur before diffusion changes.[51] Many preclinical studies have consistently shown the salvageable pH-defined penumbra, supporting the hypothesis that changes in pH are a key target with which to identify the ischemic penumbra.[46,51–56] These promising results in the preclinical setting stimulated the clinical implementation of APT-based pH imaging for stroke imaging.

4 | APT CLINICAL RESEARCH

In recent years, many groups have developed pH-sensitive APT imaging sequences on clinical scanners to improve the translation of the technique to clinical practice. The first human study was reported by Zhao et al.,[57] revealing that the APTw effect was hypointense compared with contralateral normal-appearing tissue, consistent with the findings in the preclinical studies. The APTw contrast of approximately 1% was observed when a RF saturation power of 2 μT was applied. However, the observed signal might be still contaminated by other confounding factors, such as changes in amide proton concentrations, water relaxation times, upfield NOE signals, and conventional MT asymmetry effects during the acute and subacute stages (average 4.3 ± 2.5 days after the onset of the stroke), even though the MTR asymmetry analysis was performed to remove the contribution of symmetric MT and direct water saturation effects. Later, Tee et al.[58] compared different APT imaging analysis methods (conventional MTR asymmetry versus Bayesian model-based fitting) and evaluated their pH sensitivity using hyperacute stroke patients (median 2 h 59 min after the onset of the stroke). Acidic pH is generally assumed to be the dominant contributor to APT signal contrast at the hyperacute stage, because the changes in mobile protein and peptide content, water relaxation times, and MTR asymmetry are more likely to be

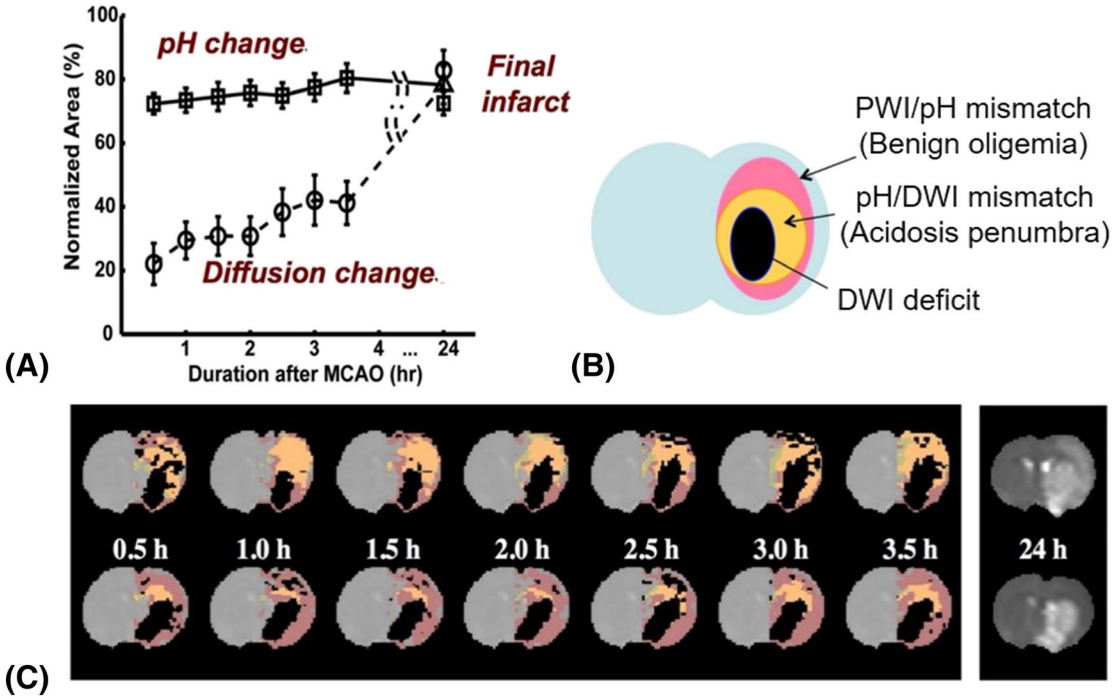

FIGURE 3 (A), Group analysis of ischemic volume evolution ($n = 18$) with a PWI–DWI mismatch, comparing areas of pH change and diffusion changes as a fraction of the perfusion deficit region. (B), Parcellation of the ischemic area in terms of three zones: a DWI deficit that will most likely proceed to infarction; a pH–DWI mismatch region at risk for infarction; and a PWI–pH mismatch not at risk. (C), Evolution of a pH deficit (orange) and a diffusion deficit (black), with regard to the perfusion deficit (purple), as a function of time after MCAO, in two rats. The T_2 image at 24 h (the right-most column in C) shows final infarction area predicted well by diffusion and pH deficit regions. (Reproduced, in part, with permission from Sun et al. *J Cereb Blood Flow Metab*. 2007;27:1129-1136)

negligible early in the evolution of ischemic stroke, as described in a previous animal study.[46] Although the APT effect measured by both analysis methods was consistently lower in the infarct core (diffusion deficit) than in contralateral normal-appearing tissue, the model-based fitting approach provided a higher APT stroke contrast-to-noise ratio and a lower variation in gray and white matter compared with the conventional asymmetry analysis, probably due to the inherent robustness of model fitting to noisy data (with outliers).[59] These early stroke patient studies showed that APT imaging in stroke patients was feasible on a 3 T clinical-field-strength scanner.

The ability to identify potential areas of reversible and salvageable brain tissue after ischemic stroke helps to identify stoke patients for intravenous, intra-arterial, or mechanical reperfusion treatment in various therapeutic windows. Harston et al.[60] demonstrated the potential clinical use of pH-sensitive APT-MRI in hyperacute ischemic stroke by assessing the relationship between intracellular pH and final tissue outcome in data from a prospective cohort of 12 patients with hyperacute ischemic stroke (median 2 h 59 min after the onset of the stroke). Importantly, within the perfusion deficit lesion, the region identified as the ischemic core (tissue present in both diffusion deficit and final FLAIR infarct) was found to have a lower APT signal, consistent with a lower pH, than the infarct growth area (ischemic penumbra, tissue present in the final FLAIR infarct, but not in the diffusion deficit). In addition, the tissue identified as benign oligemia (tissue present in the perfusion deficit, but not the final FLAIR infarct) had a significantly higher APT signal, consistent with a higher pH, than either the ischemic core or infarct growth, as shown in Figure 4. These findings suggest that the addition of pH-sensitive APT imaging to the diffusion and perfusion MRI protocol could better visualize an ischemic penumbra, thus improving predictions of final infarct size and outcome.

The APTw image contrast of the ischemic acidosis penumbra is small (~0.5%) compared with the inherent tissue signal, which limits detection sensitivity to pH. APT signals calculated from MTR asymmetry are further reduced due to the presence of NOE signals at roughly −3.5 ppm upfield from water. To separate the pH-sensitive APT effect from NOE signals, Heo et al.[61] performed a study in 30 ischemic stroke patients (<7 h after the onset of the stroke) using the so-called extrapolated semisolid magnetization transfer reference (EMR) approach.[62,63] The NOE-free APT (APT$^{\#}$) signal contrast between ischemic lesions and normal tissue was substantially increased—nearly three times larger than that based on conventional MTR asymmetry analysis—as shown in Figure 5, thus allowing the more reliable delineation of an acidotic ischemic penumbra. The patient study[61] showed that pH deficits were smaller than perfusion deficits and equal to or larger than diffusion deficits (Figure 6). Similar to the result from Harston et al.,[60] the APT deficit may reflect the area of the expected final infarction without reperfusion, and therefore the acidosis-based penumbra, in line with suggestions by Heiss, Hossmann, and Baron.[2,18,19,30] A further finding was that hyperintense APT signals were observed in hemorrhagic transformation (HT) regions as a result of abundant mobile protein and peptide contents in the blood (Figure 7), which is in agreement with the results of a previous animal study,[54] while the hypointense APT signals in ischemic lesions were primarily attributable to local tissue acidosis. These initial clinical data suggest that APT imaging is feasible for acute stroke patients and may provide extra information about the infarct in ischemic strokes, by virtue of pH changes.

After the initial successes of pH-sensitive APT imaging in stroke patients, further studies followed, such as those investigating dynamic APT signal changes in ischemic tissue at various clinical stages of stroke and correlating APT signal intensities with clinical outcome. Song et al.[64] evaluated the dynamic pH changes at the hyperacute, acute, early subacute, and late subacute stages using APTw MRI. Compared with the contralateral normal-appearing white matter, APTw signals were significantly lower in ischemic tissue for all four stages. In that study, the APTw signals of the ischemic lesion were lowest at the hyperacute stage (onset time < 6 h), but gradually increased from the onset time, suggesting that the tissue acidification in the ischemic tissue may decrease with time from stoke onset. However, the pH contribution to the APTw signals might also vary with time and with changes in upfield NOE signals and water relaxation times due to the development of cytotoxic and vasogenic edema. All

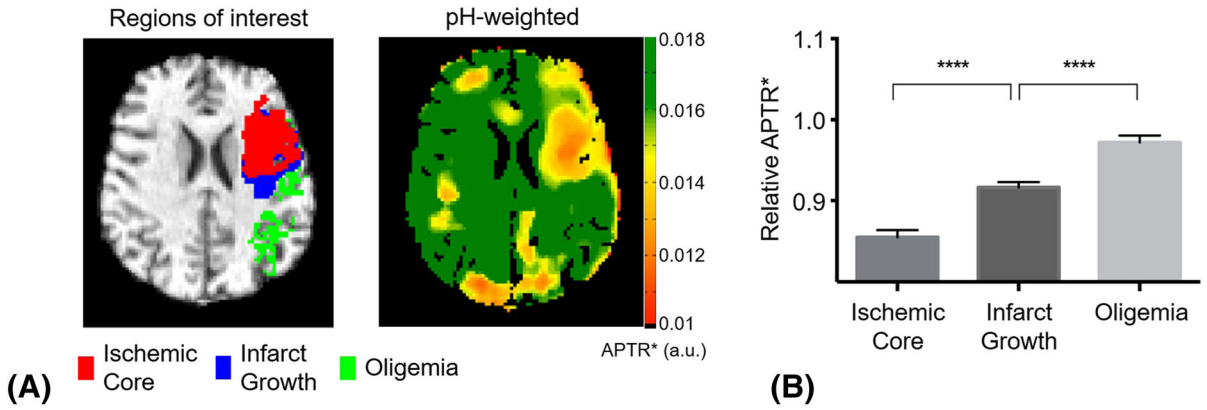

FIGURE 4 (A), Quantified APT effect in the ischemic core, infarct growth, and oligemia region of a representative hyperacute stroke patient. (B), The mean relative APTR* (relative to the contralateral normal brain tissue) shows significant differences between the different regions of interest, where the error bars represent 95% confidence intervals and **** $P < 0.0001$. (Reproduced, in part, with permission from Harston et al. *Brain*. 2015;138:36-42)

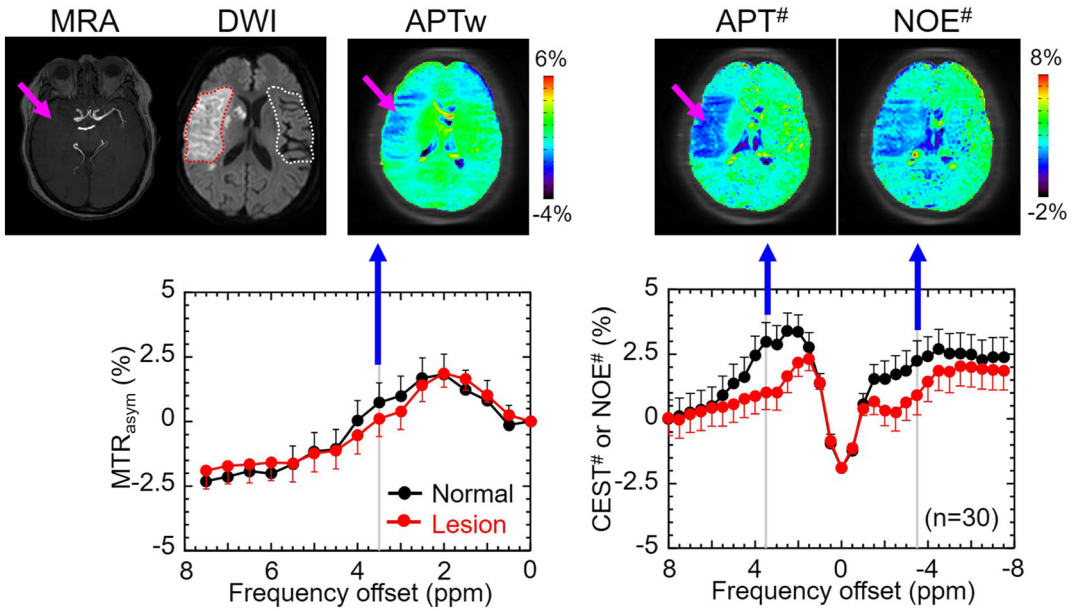

FIGURE 5 Conventional MR angiography, DWI, APTw, APT$^{\#}$, and NOE$^{\#}$ images from an acute stroke patient (<7 h from symptom onset) with a right MCA occlusion (magenta arrows). Two regions of interest, an ischemic lesion that was DWI hyperintense (red dotted line on DWI) and contralateral normal tissue (white dotted line on DWI) were drawn. While APTw-MRI for pH analysis was confounded by upfield NOE effects of mobile proteins and peptides, the NOE-free APT$^{\#}$ contrast between normal and ischemic lesions was substantially increased, nearly three times more than that based on MTR_{asym} analysis. The APT$^{\#}$ signal contrast (−1.45 ± 0.4%) was significantly larger than the APTw signal contrast (−0.39 ± 0.5%, $P < 0.001$). (Reproduced, in part, with permission from Heo et al. *Magn Reson Med*. 2017;78:871-880)

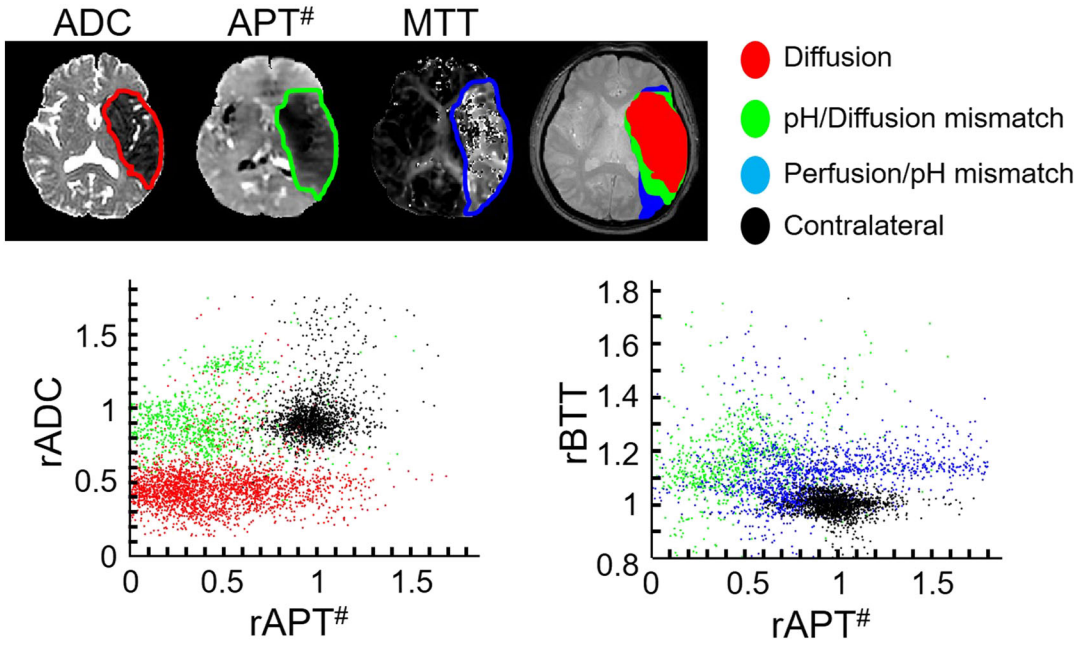

FIGURE 6 Comparison of diffusion, pH, and perfusion deficits and quantitative pH–diffusion and perfusion–pH scatterplots in an acute stroke patient. Of the 13 patients scanned at the acute phase (<7 h), three patients showed an acidosis-based ischemic penumbra. The distributions of the diffusion deficit area (infarct core, red), pH–diffusion mismatch (acidosis-based penumbra, green), and perfusion–pH mismatch (acidosis-based benign oligemia, blue) were markedly different from those of the contralateral normal tissue (black). (Reproduced, in part, with permission from Heo et al. *Magn Reson Med*. 2017;78:871-880)

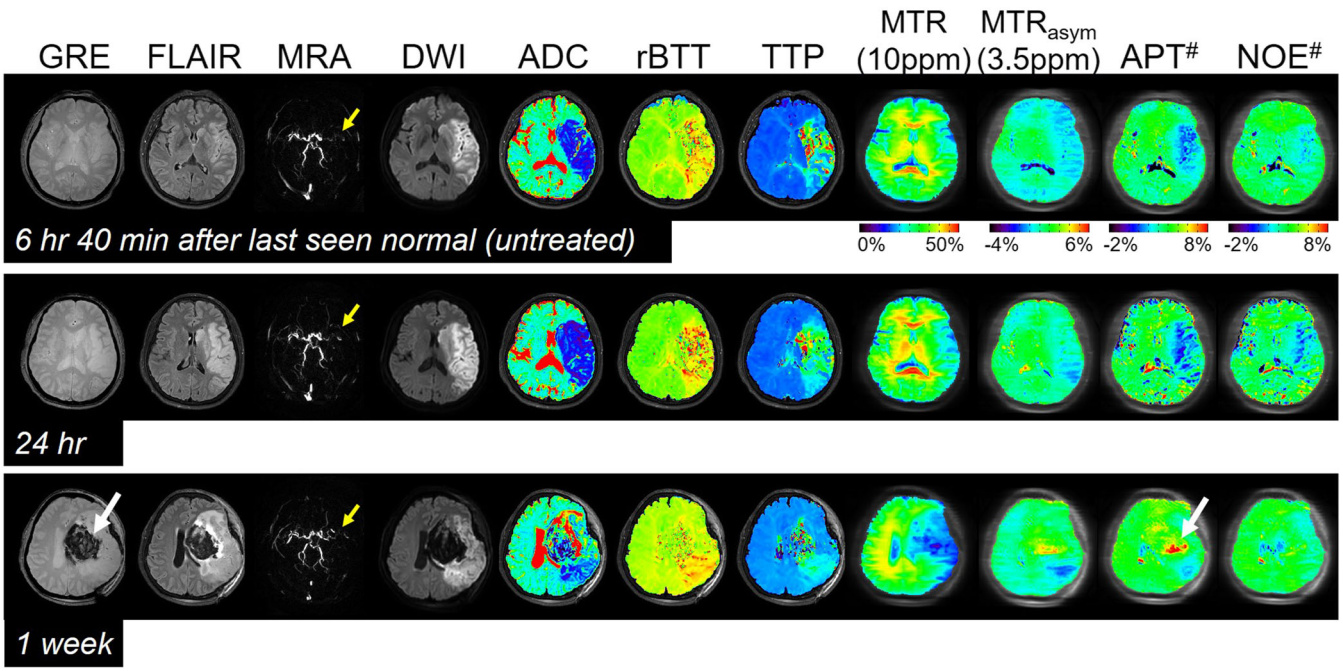

FIGURE 7 Serial multimodality MR images of a representative acute stroke patient with a left MCA occlusion (yellow arrows) at three time points. The DWI and ADC showed large, acute ischemic areas caused by cytotoxic edema. In addition, perfusion-based relative bolus transit time (rBTT) and time to peak (TTP) showed obvious hypoperfusion in a slightly larger region than the diffusion abnormality. The high APT signal intensities observed at one week can be attributed to a hemorrhage (white arrows) caused by abundant mobile proteins and peptides in the blood. The patient presented outside of a treatment time window, did not receive an acute intervention, and subsequently suffered a spontaneous symptomatic hemorrhagic transformation of the ischemic infarct. (Reproduced, in part, with permission from Heo et al. *Magn Reson Med*. 2017;78:871-880)

these different contributions are highly dependent on the RF saturation parameters[65,66] used in the CEST acquisition, and thus it has not been possible to date to resolve these different contributions across the studies performed in patients.

Lin et al.[67] and Momosaka et al.[68] investigated the correlation between APTw signals and clinical stroke severity using the National Institutes of Health Stroke Scale (NIHSS), and the prognosis with the 90 day modified Rankin scale (mRS) score. Both studies showed that the APTw signal was significantly inversely correlated with the NIHSS score. More importantly, the APTw signal within an infarct lesion was significantly lower in the poor prognosis group (mRS score > 2) than in the good prognosis group (mRS score < 2). Furthermore, Yu et al.[69] assessed the therapeutic efficacy of supportive treatments in ischemic stroke patients using APTw MRI. Forty-three ischemic patients (median 3 days after the onset of the stroke) who were not suitable for thrombolysis, and underwent only supportive treatment that included antiplatelet and anticoagulation therapy and free radical scavenging, were imaged by APTw MRI prior to treatment and underwent follow-up scans after treatment. The APTw signal contrast between ischemic lesions and contralateral normal-appearing white matter tissues had significant correlations with the NIHSS at arrival. Most of the ischemic stroke patients (24 of 26 patients) showed progressively increased APTw signal intensities in the ischemic lesion over all time points after treatment, with improvements in clinical symptoms and thus the NIHSS. Although the clinical results should be interpreted with caution due to the small sample size of the studies and the inclusion of heterogeneous populations, the findings described above raise the intriguing possibility that pH-sensitive APT imaging could be used to assess stroke severity and the therapeutic effect of ischemic stroke treatments, and in the prediction of long-term clinical outcome for ischemic stroke patients.

5 | DISCUSSION

To date, clinical studies of ischemic stroke appear to agree with preclinical work, which has demonstrated that the APT signal intensity in ischemic tissue is lower compared with normal, healthy tissue in early stroke imaging.[41,42] The reduced APT signal has been widely hypothesized to be the result of tissue acidosis due to lactic acid accumulation by enhancing anaerobic glycolysis. This acidosis hypothesis seems most likely to be valid in the early hyperacute phase, where there has been less time for additional tissue changes to occur that might affect other contributors to the APT signal. Various clinical studies have included ischemic stroke patients who were scanned days after the onset of the stroke.[67,69] These studies found that the APT signal within the ischemic lesion gradually increased as time progressed from symptom onset, and yet the ischemic region still

showed a significant difference when compared with the normal tissue area. One of these studies even reported that the APT signal in the ischemic lesion became hyperintense when imaged one week after the onset of the stroke. It is currently premature to ascribe a pH change as the main contributing factor to the decreased or increased APT signal observed in the days immediately after stroke. A cascade of physiological changes occur after stroke; thus, relating the APT signal change to a pH drop or to normalization may not be warranted, especially in the late stage of stroke.[70–75] Many physiological changes, such as protein disintegration, edema, and inflammation, have been observed after stroke, which likely influence APT signals. As a result, more work is required to investigate the exact source(s) or pathway(s) that led to the current observations.

One of the main limitations faced by APT clinical studies is the recruitment of stroke patients. This is especially challenging in the hyperacute setting, where patients can find it difficult to tolerate research MRI scans and early evaluation and treatment are time critical. In addition to this, follow-up imaging is also difficult to acquire because one in eight strokes are fatal within the first 30 days and almost two-thirds of strokes lead to disability. As a result, the follow-up recruitment to confirm APT findings is often incomplete or leads to the use of inconsistent final infarct definitions. This particularly affects studies that target the investigation of APT effect across different stroke time points.

In addition, there are several technical hurdles in the clinical translation of APT-MRI. These include a relatively long scan time because of the use of a long RF saturation pulse per frequency offset, and a series of saturation frequencies that must be acquired to form a *Z*-spectrum. The American Heart Association (AHA) recommends that imaging occur within 25 min of emergency department (ED) arrival and that interpretation of imaging should occur within 45 min of ED arrival. There is, thus, only a 20 min time window in which to acquire and interpret the images.[76–78] A long APT imaging can lead to more motion artifacts in restless patients, which can produce unusable images, wasting precious minutes. For improvement in acquisition speed, APT imaging could be combined with advanced fast imaging technologies, including reduced *k*-space sampling with parallel imaging,[79,80] compressed sensing[81–83] and MR fingerprinting.[84–89] Importantly, quick image reconstruction, in addition to imaging acquisition, is essential for clinical translation. The development of real-time, pH–diffusion mismatch analysis software for unsupervised and fully automated processing on scanners is, therefore, highly desired. A faster APT scan not only would help to improve patient comfort and compliance, but also could be used to improve image quality. Furthermore, higher spatial resolution and volumetric 3D imaging would be valuable for the more precise depiction of an acidosis-based penumbra.

There remains some uncertainty regarding pH specificity of APT MRI in ischemic lesions. APT contrast is believed to be predominantly driven by ischemic acidosis during the very early stages of ischemia, where water content and relaxation weighted images may not show contrast. However, as previous studies indicate,[58,90] vasogenic edema begins to develop during the first 24 to 48 h after the onset of a stroke, and alters the magnetic properties of water and causes a change in the diffusivity in the ischemic area, which affects water content and T_1 and T_2 relaxation times, all of which can also influence APT contrast. Another possible issue is the possible contribution of other CEST signals to APT contrast, such as signals from faster exchanging protons, such as on amine and guanidinium. However, CEST effects are dominated by the slowly exchanging amide protons at lower RF saturation powers, with faster-exchanging protons contributing at higher RF saturation powers. Therefore, employing a low-power RF saturation may be sufficient to avoid contributions from the rapidly exchangeable protons that occur at the APT frequency. CEST specificity is expected to increase at higher magnetic field strength (7 T) due to high spectral resolution. However, ultrahigh-field 7 T machines are not accessible for most acute clinical applications, and MRI as a first-line imaging modality is currently still limited to standard (1.5 T) and high (3 T) field strength MRI. New APT imaging techniques have been developed to correct water relaxation and multiple overlapping CEST effects, improving pH specificity, but have not yet been demonstrated in stroke patient studies.[91–94] Other potential factors affecting APT signals are static magnetic field (B_0) and RF field (B_1) inhomogeneities, which cause a shift in the water resonance frequency and spatial variation in labeling efficiency, respectively. Several correction methods have been developed to mitigate the effect of the field inhomogeneities on APT images.[95,96]

A standardized APT imaging protocol is necessary for the proper design of prospective, population-based studies of acute stroke, which includes RF saturation parameters, imaging acquisition schemes, and image analysis methods. Although the first clinical study by Zhao et al.[57] aimed to propose an optimal RF saturation power parameter for APT imaging of stroke with limited hardware (e.g., RF amplifiers and transmitter/receiver RF coils) performance, further investigations of the standardization of scan parameters and imaging sequences to enhance the pH specificity and sensitivity are needed. In addition, the post-processing methods used for APT-MRI are not standardized. Several previous studies have demonstrated that various analysis methods can lead to variation in APT signal intensities or contrast between ischemic and normal tissues,[58,61,97] as shown in Figure 8.[98] Therefore, standardization of APT image analysis is necessary for the incorporation of this analysis into clinical studies and the promotion of its use in clinical trials and clinical practice.

Despite the challenges of using MRI to triage acute stroke patients, there is a growing movement to expand its use. It is possible to meet the time metrics specified in the AHA guidelines[99,100] because MRI can exclude stroke mimics, thereby avoiding unnecessary and inappropriate administration of thrombolysis, which is costly and can be harmful. MRI is currently used to triage patients who present in an unknown window.[37,101] Although it has been shown that CT triage does not benefit stroke patients who present with non-disabling deficits, it appears that MRI may be able to identify a population that would benefit.[102,103] Thus, adding APT imaging to current clinical sequences could further enhance its ability to expand treatment options. For instance, the APT-based penumbra would be the first and only way to identify at-risk tissue without exogenous contrast, the administration of which is not always possible or successful. Another potential key application is the differentiation of atheromatous-based vessel occlusion from embolic-based vessel occlusion, with the former more likely to result in a chronic perfusion deficit (without a change in pH), indicating a target that may be less amenable to mechanical thrombectomy. Thus, as MRI becomes a more commonly

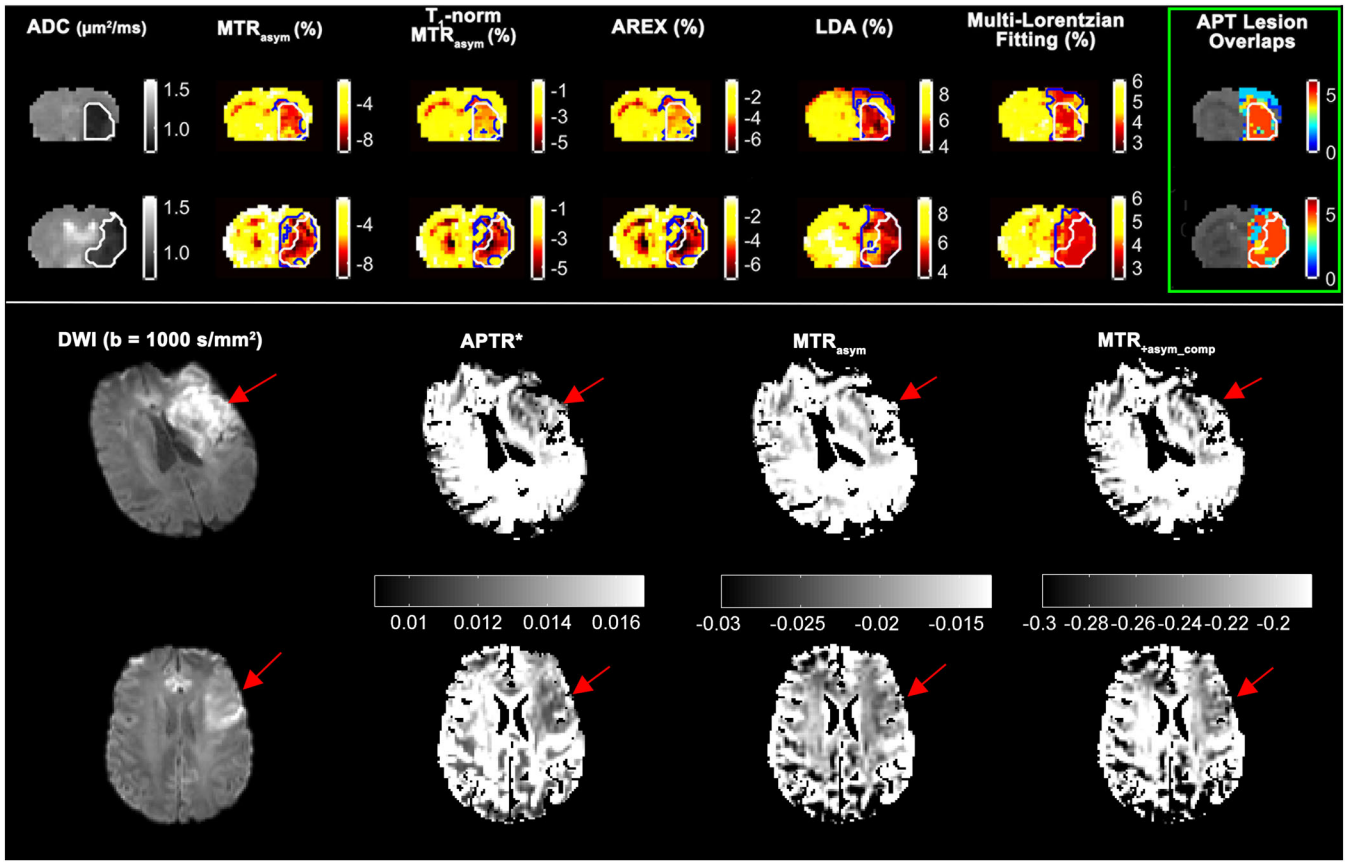

FIGURE 8 Representative results from an animal (top two rows) and an ischemic stroke patient (bottom two rows) quantified using some of the common analysis methods (MTR$_{aysm}$, T_1-norm MTR$_{asym}$, AREX, LDA, multi-Lorentzian fitting, APTR*, MTR$_{asym_comp}$). It is obvious from the results that different analysis methods produce different ischemic areas, as highlighted by the green rectangular box and red arrows, but they all show significant differences when compared with the contralateral normal-appearing tissue. The animal results (top two rows) are reproduced, in part, with permission from Foo et al. *Magn Reson Med*. 2021;85:2188-2200 and the patient results (bottom two rows) are reproduced, in part, with permission from Tee et al. *NMR Biomed*. 2014;27(9):1019-1029

used modality in the acute stroke field, it is important that APT methodologies are ready to be integrated into clinical practice. In addition, recent preclinical and clinical studies have shown that APT-MRI is capable of detecting and differentiating hemorrhage stroke (increased concentration of mobile protein in blood, showing hyperintensity with respect to normal tissue) from ischemic stroke (decreased pH due to tissue acidosis, showing hypointensity).[54,61,104,105] Although it may be premature to declare that APT-MRI is as good as CT or conventional T_1w/T_2w MRI for the detection of hemorrhage in acute stroke patients, APT-MRI alone would provide the simultaneous visualization and separation of hemorrhagic and ischemic stroke at the hyperacute stage, substantially simplifying stroke patient management.

6 | CONCLUSIONS

The majority of the reported findings in preclinical and clinical studies have highlighted the potential of APT imaging to revolutionize clinical stroke imaging. This can potentially lead to better diagnosis and stratification of ischemic stroke patients for thrombolysis and thrombectomy, although larger clinical trials and further developments are still required to validate the clinical opportunity offered by translating APT imaging into clinical stroke practice. The addition of APT-based imaging to the standard MRI protocol could better visualize an ischemic penumbra, thereby identifying patients for whom thrombolytic therapy is appropriate, even if their clinical course lies outside the conventionally defined time window.

ORCID

Hye-Young Heo https://orcid.org/0000-0002-7297-2015

Yee Kai Tee https://orcid.org/0000-0002-0263-6358

REFERENCES

1. Astrup J, Siesjo BK, Symon L. Thresholds in cerebral ischemia—the ischemic penumbra. *Stroke*. 1981;12(6):723-725. doi:10.1161/01.STR.12.6.723
2. Hossmann KA. Viability thresholds and the penumbra of focal ischemia. *Ann Neurol*. 1994;36(4):557-565. doi:10.1002/ana.410360404
3. Heiss WD. Ischemic penumbra: evidence from functional imaging in man. *J Cereb Blood Flow Metab*. 2000;20(9):1276-1293. doi:10.1097/00004647-200009000-00002
4. Baron JC, Bousser MG, Rey A, Guillard A, Comar D, Castaigne P. Reversal of focal "misery-perfusion syndrome" by extra-intracranial arterial bypass in hemodynamic cerebral ischemia. A case study with ^{15}O positron emission tomography. *Stroke*. 1981;12(4):454-459. doi:10.1161/01.STR.12.4.454
5. Warach S, Dashe JF, Edelman RR. Clinical outcome in ischemic stroke predicted by early diffusion-weighted and perfusion magnetic resonance imaging: a preliminary analysis. *J Cereb Blood Flow Metab*. 1996;16(1):53-59. doi:10.1097/00004647-199601000-00006
6. Barber PA, Darby DG, Desmond PM, et al. Prediction of stroke outcome with echoplanar perfusion- and diffusion-weighted MRI. *Neurology*. 1998;51(2):418-426. doi:10.1212/WNL.51.2.418
7. Schwamm LH, Koroshetz WJ, Sorensen AG, et al. Time course of lesion development in patients with acute stroke: serial diffusion- and hemodynamic-weighted magnetic resonance imaging. *Stroke*. 1998;29(11):2268-2276. doi:10.1161/01.STR.29.11.2268
8. Neumann-Haefelin T, Wittsack HJ, Wenserski F, et al. Diffusion- and perfusion-weighted MRI—the DWI/PWI mismatch region in acute stroke. *Stroke*. 1999;30(8):1591-1597. doi:10.1161/01.STR.30.8.1591
9. Saver JL, Fonarow GC, Smith EE, et al. Time to treatment with intravenous tissue plasminogen activator and outcome from acute ischemic stroke. *J Am Med Assoc*. 2013;309(23):2480-2488. doi:10.1001/jama.2013.6959
10. Donnan GA, Davis SM. Neuroimaging, the ischaemic penumbra, and selection of patients for acute stroke therapy. *Lancet Neurol*. 2002;1(7):417-425. doi:10.1016/S1474-4422(02)00189-8
11. Hacke W, Donnan G, Fieschi C, et al. Association of outcome with early stroke treatment: pooled analysis of ATLANTIS, ECASS, and NINDS rt-PA stroke trials. *Lancet*. 2004;363(9411):768-774. doi:10.1016/S0140-6736(04)15692-4
12. Schellinger PD, Warach S. Therapeutic time window of thrombolytic therapy following stroke. *Curr Atheroscler Rep*. 2004;6(4):288-294. doi:10.1007/s11883-004-0060-3
13. Albers GW. Late window paradox. *Stroke*. 2018;49(3):768-771. doi:10.1161/STROKEAHA.117.020200
14. Albers GW, Marks MP, Kemp S, et al. Thrombectomy for stroke at 6 to 16 hours with selection by perfusion imaging. *N Engl J Med*. 2018;378(8):708-718. doi:10.1056/NEJMoa1713973
15. Nogueira RG, Jadhav AP, Haussen DC, et al. Thrombectomy 6 to 24 hours after stroke with a mismatch between deficit and infarct. *N Engl J Med*. 2018;378(1):11-21. doi:10.1056/NEJMoa1706442
16. Ma H, Campbell BCV, Parsons MW, et al. Thrombolysis guided by perfusion imaging up to 9 hours after onset of stroke. *N Engl J Med*. 2019;380(19):1795-1803. doi:10.1056/NEJMoa1813046
17. Baron JC. Mapping the ischaemic penumbra with PET: a new approach. *Brain*. 2001;124(1):2-4. doi:10.1093/brain/124.1.2
18. Heiss WD. The concept of the penumbra: can it be translated to stroke management? *Int J Stroke*. 2010;5(4):290-295. doi:10.1111/j.1747-4949.2010.00444.x
19. Baron JC. Perfusion thresholds in human cerebral ischemia: historical perspective and therapeutic implications. *Cerebrovasc Dis*. 2001;11(Suppl 1):2-8. doi:10.1159/000049119
20. Campbell BC, Purushotham A, Christensen S, et al. The infarct core is well represented by the acute diffusion lesion: sustained reversal is infrequent. *J Cereb Blood Flow Metab*. 2012;32(1):50-56. doi:10.1038/jcbfm.2011.102
21. Chemmanam T, Campbell BC, Christensen S, et al. Ischemic diffusion lesion reversal is uncommon and rarely alters perfusion–diffusion mismatch. *Neurology*. 2010;75(12):1040-1047. doi:10.1212/WNL.0b013e3181f39ab6
22. Pexman JH, Barber PA, Hill MD, et al. Use of the Alberta Stroke Program Early CT Score (ASPECTS) for assessing CT scans in patients with acute stroke. *Am J Neuroradiol*. 2001;22(8):1534-1542.
23. Tatlisumak T. Is CT or MRI the method of choice for imaging patients with acute stroke? Why should men divide if fate has united. *Stroke*. 2002;33(9):2144-2145. doi:10.1161/01.STR.0000026862.42440.AA
24. Albers GW, Thijs VN, Wechsle L, et al. Magnetic resonance imaging profiles predict clinical response to early reperfusion: The diffusion and perfusion imaging evaluation for understanding stroke evolution (DEFUSE) study. *Ann Neurol*. 2006;60(5):508-517. doi:10.1002/ana.20976
25. Schlaug G, Benfield A, Baird AE, et al. The ischemic penumbra—operationally defined by diffusion and perfusion MRI. *Neurology*. 1999;53(7):1528-1537. doi:10.1212/WNL.53.7.1528
26. Gonzalez RG, Schaefer PW, Buonanno FS, et al. Diffusion-weighted MR imaging: diagnostic accuracy in patients imaged within 6 hours of stroke symptom onset. *Radiology*. 1999;210(1):155-162. doi:10.1148/radiology.210.1.r99ja02155
27. Chalela JA, Kidwell CS, Nentwich LM, et al. Magnetic resonance imaging and computed tomography in emergency assessment of patients with suspected acute stroke: a prospective comparison. *Lancet*. 2007;369(9558):293-298. doi:10.1016/S0140-6736(07)60151-2
28. Morita S, Suzuki M, Iizuka K. False-negative diffusion-weighted MRI in acute cerebellar stroke. *Auris Nasus Larynx*. 2011;38(5):577-582. doi:10.1016/j.anl.2011.01.017
29. Kucinski T, Naumann D, Knab R, et al. Tissue at risk is overestimated in perfusion weighted imaging: MR imaging in acute stroke patients without vessel recanalization. *Am J Neuroradiol*. 2005;26(4):815-819.
30. Hossmann KA. Pathophysiological basis of translational stroke research. *Folia Neuropathol*. 2009;47(3):213-227.
31. Guadagno JV, Donnan GA, Markus R, Gillard JH, Baron JC. Imaging the ischaemic penumbra. *Curr Opin Neurol*. 2004;17(1):61-67. doi:10.1097/00019052-200402000-00011
32. Schaefer PW, Barak ER, Kamalian S, et al. Quantitative assessment of core/penumbra mismatch in acute stroke: CT and MR perfusion imaging are strongly correlated when sufficient brain volume is imaged. *Stroke*. 2008;39(11):2986-2992. doi:10.1161/STROKEAHA.107.513358
33. Parsons MW, Yang Q, Barber PA, et al. Perfusion magnetic resonance imaging maps in hyperacute stroke: relative cerebral blood flow most accurately identifies tissue destined to infarct. *Stroke*. 2001;32(7):1581-1587. doi:10.1161/01.STR.32.7.1581
34. Grandin CB, Duprez TP, Smith AM, et al. Usefulness of magnetic resonance-derived quantitative measurements of cerebral blood flow and volume in prediction of infarct growth in hyperacute stroke. *Stroke*. 2001;32(5):1147-1153. doi:10.1161/01.STR.32.5.1147

35. Coutts SB, Simon JE, Tomanek AI, et al. Reliability of assessing percentage of diffusion-perfusion mismatch. *Stroke*. 2003;34(7):1681-1683. doi:10.1161/01.STR.0000078840.96473.20
36. Yoo AJ, Barak ER, Copen WA, et al. Combining acute diffusion-weighted imaging and mean transmit time lesion volumes with National Institutes of Health Stroke Scale Score improves the prediction of acute stroke outcome. *Stroke*. 2010;41(8):1728-1735. doi:10.1161/STROKEAHA.110.582874
37. Thomalla G, Simonsen CZ, Boutitie F, et al. MRI-guided thrombolysis for stroke with unknown time of onset. *N Engl J Med*. 2018;379(7):611-622. doi:10.1056/NEJMoa1804355
38. Pfaff JA, Bendszus M, Donnan G, et al. The impact of the DWI-FLAIR-mismatch in the ECASS-4 trial—a post hoc analysis. *Eur Stroke J*. 2020;5(4):370-373. doi:10.1177/2396987320920114
39. van Zijl PCM, Yadav NN. Chemical exchange saturation transfer (CEST): what is in a name and what isn't? *Magn Reson Med*. 2011;65(4):927-948. doi:10.1002/mrm.22761
40. Zhou J, Heo HY, Knutsson L, van Zijl PCM, Jiang S. APT-weighted MRI: techniques, current neuro applications, and challenging issues. *J Magn Reson Imaging*. 2019;50(2):347-364. doi:10.1002/jmri.26645
41. Leigh R, Knutsson L, Zhou J, van Zijl PC. Imaging the physiological evolution of the ischemic penumbra in acute ischemic stroke. *J Cereb Blood Flow Metab*. 2017;38(9):1500-1516. doi:10.1177/0271678X17700913
42. Foo LS, Harston G, Mehndiratta A, et al. Clinical translation of amide proton transfer (APT) MRI for ischemic stroke: a systematic review (2003–2020). *Quant Imaging Med Surg*. 2021;11(8):3797-3811. doi:10.21037/qims-20-1339
43. Davis D, Ulatowski J, Eleff S, et al. Rapid monitoring of changes in water diffusion coefficients during reversible ischemia in cat and rat brain. *Magn Reson Med*. 1994;31(4):454-460. doi:10.1002/mrm.1910310416
44. Minematsu K, Li L, Sotak CH, Davis MA, Fisher M. Reversible focal ischemic injury demonstrated by diffusion-weighted magnetic resonance imaging in rats. *Stroke*. 1992;23(9):1304-1310; discussion 1310-1301. doi:10.1161/01.STR.23.9.1304
45. Siesjo BK. Pathophysiology and treatment of focal cerebral ischemia. *J Neurosurg*. 1992;77(3):337-354. doi:10.3171/jns.1992.77.3.0337
46. Zhou J, Payen J, Wilson DA, Traystman RJ, van Zijl PCM. Using the amide proton signals of intracellular proteins and peptides to detect pH effects in MRI. *Nat Med*. 2003;9(8):1085-1090. doi:10.1038/nm907
47. Zhou J, Wilson DA, Sun PZ, Klaus JA, Van Zijl PCM. Quantitative description of proton exchange processes between water and endogenous and exogenous agents for WEX, CEST, and APT experiments. *Magn Reson Med*. 2004;51(5):945-952. doi:10.1002/mrm.20048
48. Vinogradov E, Sherry AD, Lenkinski RE. CEST: from basic principles to applications, challenges and opportunities. *J Magn Reson*. 2013;229:155-172. doi:10.1016/j.jmr.2012.11.024
49. Wuthrich K. *NMR of Proteins and Nucleic Acids*. Vol. 17. Wiley; 1986:11-13. doi:10.1051/epn/19861701011.
50. Englander SW, Downer NW, Teitelbaum H. Hydrogen exchange. *Annu Rev Biochem*. 1972;41(1):903-924. doi:10.1146/annurev.bi.41.070172.004351
51. Sun PZ, Zhou J, Sun W, Huang J, van Zijl PCM. Detection of the ischemic penumbra using pH-weighted MRI. *J Cereb Blood Flow Metab*. 2007;27(6):1129-1136. doi:10.1038/sj.jcbfm.9600424
52. Guo Y, Zhou IY, Chan ST, et al. pH-sensitive MRI demarcates graded tissue acidification during acute stroke—pH specificity enhancement with magnetization transfer and relaxation-normalized amide proton transfer (APT) MRI. *NeuroImage*. 2016;141:242-249. doi:10.1016/j.neuroimage.2016.07.025
53. Jin T, Wang P, Zong XP, Kim SG. Magnetic resonance imaging of the Amine-Proton EXchange (APEX) dependent contrast. *Neuroimage*. 2012;59(2):1218-1227. doi:10.1016/j.neuroimage.2011.08.014
54. Wang M, Hong X, Chang CF, et al. Simultaneous detection and separation of hyperacute intracerebral hemorrhage and cerebral ischemia using amide proton transfer MRI. *Magn Reson Med*. 2015;74(1):42-50. doi:10.1002/mrm.25690
55. Sun PZ, Murata Y, Lu J, Wang X, Lo EH, Sorensen AG. Relaxation-compensated fast multislice amide proton transfer (APT) imaging of acute ischemic stroke. *Magn Reson Med*. 2008;59(5):1175-1182. doi:10.1002/mrm.21591
56. Sun PZ, Zhou J, Huang J, van Zijl P. Simplified quantitative description of amide proton transfer (APT) imaging during acute ischemia. *Magn Reson Med*. 2007;57(2):405-410. doi:10.1002/mrm.21151
57. Zhao X, Wen Z, Huang F, et al. Saturation power dependence of amide proton transfer image contrasts in human brain tumors and strokes at 3 T. *Magn Reson Med*. 2011;66(4):1033-1041. doi:10.1002/mrm.22891
58. Tee YK, Harston GW, Blockley N, et al. Comparing different analysis methods for quantifying the MRI amide proton transfer (APT) effect in hyperacute stroke patients. *NMR Biomed*. 2014;27(9):1019-1029. doi:10.1002/nbm.3147
59. Chappell MA, Donahue MJ, Tee YK, et al. Quantitative Bayesian model-based analysis of amide proton transfer MRI. *Magn Reson Med*. 2013;70(2):556-567. doi:10.1002/mrm.24474
60. Harston GW, Tee YK, Blockley N, et al. Identifying the ischaemic penumbra using pH-weighted magnetic resonance imaging. *Brain*. 2015;138(1):36-42. doi:10.1093/brain/awu374
61. Heo HY, Zhang Y, Burton TM, et al. Improving the detection sensitivity of pH-weighted amide proton transfer MRI in acute stroke patients using extrapolated semisolid magnetization transfer reference signals. *Magn Reson Med*. 2017;78(3):871-880. doi:10.1002/mrm.26799
62. Heo HY, Zhang Y, Jiang S, Lee DH, Zhou J. Quantitative assessment of amide proton transfer (APT) and nuclear Overhauser enhancement (NOE) imaging with extrapolated semisolid magnetization transfer reference (EMR) signals: II. Comparison of three EMR models and application to human brain glioma at 3 Tesla. *Magn Reson Med*. 2016;75(4):1630-1639. doi:10.1002/mrm.25795
63. Heo HY, Zhang Y, Lee DH, Hong X, Zhou J. Quantitative assessment of amide proton transfer (APT) and nuclear Overhauser enhancement (NOE) imaging with extrapolated semi-solid magnetization transfer reference (EMR) signals: Application to a rat glioma model at 4.7 tesla. *Magn Reson Med*. 2016;75(1):137-149. doi:10.1002/mrm.25581
64. Song G, Li C, Luo X, et al. Evolution of cerebral ischemia assessed by amide proton transfer-weighted MRI. *Front Neurol*. 2017;8:67. doi:10.3389/fneur.2017.00067
65. Heo HY, Lee DH, Zhang Y, et al. Insight into the quantitative metrics of chemical exchange saturation transfer (CEST) imaging. *Magn Reson Med*. 2017;77(5):1853-1865. doi:10.1002/mrm.26264
66. Heo HY, Zhang Y, Jiang S, Zhou J. Influences of experimental parameters on chemical exchange saturation transfer (CEST) metrics of brain tumors using animal models at 4.7T. *Magn Reson Med*. 2019;81(1):316-330. doi:10.1002/mrm.27389

67. Lin G, Zhuang C, Shen Z, et al. APT weighted MRI as an effective imaging protocol to predict clinical outcome after acute ischemic stroke. *Front Neurol*. 2018;9:901. doi:10.3389/fneur.2018.00901
68. Momosaka D, Togao O, Kikuchi K, Kikuchi Y, Wakisaka Y, Hiwatashi A. Correlations of amide proton transfer-weighted MRI of cerebral infarction with clinico-radiological findings. *PLoS ONE*. 2020;15(8):e0237358. doi:10.1371/journal.pone.0237358
69. Yu L, Chen Y, Chen M, et al. Amide proton transfer MRI signal as a surrogate biomarker of ischemic stroke recovery in patients with supportive treatment. *Front Neurol*. 2019;10:104. doi:10.3389/fneur.2019.00104
70. de Courten-Myers GM, Kleinholz M, Holm P, et al. Hemorrhagic infarct conversion in experimental stroke. *Ann Emerg Med*. 1992;21(2):120-126. doi:10.1016/S0196-0644(05)80144-1
71. Zollner JP, Hattingen E, Singer OC, Pilatus U. Changes of pH and energy state in subacute human ischemia assessed by multinuclear magnetic resonance spectroscopy. *Stroke*. 2015;46(2):441-446. doi:10.1161/STROKEAHA.114.007896
72. Venkat P, Chopp M, Chen J. Blood–brain barrier disruption, vascular impairment, and ischemia/reperfusion damage in diabetic stroke. *J Am Heart Assoc*. 2017;6(6). doi:10.1161/JAHA.117.005819
73. Song EC, Chu K, Jeong SW, et al. Hyperglycemia exacerbates brain edema and perihematomal cell death after intracerebral hemorrhage. *Stroke*. 2003;34(9):2215-2220. doi:10.1161/01.STR.0000088060.83709.2C
74. Pulsinelli WA, Waldman S, Rawlinson D, Plum F. Moderate hyperglycemia augments ischemic brain damage: a neuropathologic study in the rat. *Neurology*. 1982;32(11):1239-1246. doi:10.1212/WNL.32.11.1239
75. Dietrich WD, Alonso O, Busto R. Moderate hyperglycemia worsens acute blood–brain barrier injury after forebrain ischemia in rats. *Stroke*. 1993;24(1):111-116. doi:10.1161/01.STR.24.1.111
76. European Stroke Organisation (ESO) Executive Committee and ESO Writing Committee. Guidelines for Management of Ischaemic Stroke and Transient Ischaemic Attack 2008. *Cerebrovasc Dis*. 2008;25(5):457-507. doi:10.1159/000131083
77. Saver JL. Time is brain—quantified. *Stroke*. 2006;37(1):263-266. doi:10.1161/01.STR.0000196957.55928.ab
78. Wahlgren N, Ahmed N, Eriksson N, et al. Multivariable analysis of outcome predictors and adjustment of main outcome results to baseline data profile in randomized controlled trials: Safe Implementation of Thrombolysis in Stroke-MOnitoring STudy (SITS-MOST). *Stroke*. 2008;39(12):3316-3322. doi:10.1161/STROKEAHA.107.510768
79. Zhang Y, Heo HY, Jiang S, Zhou J, Bottomley PA. Fast 3D chemical exchange saturation transfer imaging with variably-accelerated sensitivity encoding (vSENSE). *Magn Reson Med*. 2019;82(6):2046-2061. doi:10.1002/mrm.27881
80. Zhang Y, Heo HY, Lee DH, et al. Chemical exchange saturation transfer (CEST) imaging with fast variably-accelerated sensitivity encoding (vSENSE). *Magn Reson Med*. 2017;77(6):2225-2238. doi:10.1002/mrm.26307
81. Heo HY, Xu X, Jiang S, et al. Prospective acceleration of parallel RF transmission-based 3D chemical exchange saturation transfer imaging with compressed sensing. *Magn Reson Med*. 2019;82(5):1812-1821. doi:10.1002/mrm.27875
82. Heo HY, Zhang Y, Lee DH, Jiang S, Zhao X, Zhou J. Accelerating chemical exchange saturation transfer (CEST) MRI by combining compressed sensing and sensitivity encoding techniques. *Magn Reson Med*. 2017;77(2):779-786. doi:10.1002/mrm.26141
83. Lustig M, Donoho D, Pauly JM. Sparse MRI: the application of compressed sensing for rapid MR imaging. *Magn Reson Med*. 2007;58(6):1182-1195. doi:10.1002/mrm.21391
84. Ma D, Gulani V, Seiberlich N, et al. Magnetic resonance fingerprinting. *Nature*. 2013;495(7440):187-192. doi:10.1038/nature11971
85. Heo HY, Han Z, Jiang S, Schar M, van Zijl PCM, Zhou J. Quantifying amide proton exchange rate and concentration in chemical exchange saturation transfer imaging of the human brain. *NeuroImage*. 2019;189(1):202-213. doi:10.1016/j.neuroimage.2019.01.034
86. Kim B, Schar M, Park H, Heo HY. A deep learning approach for magnetization transfer contrast MR fingerprinting and chemical exchange saturation transfer imaging. *NeuroImage*. 2020;221:117165. doi:10.1016/j.neuroimage.2020.117165
87. Kang B, Kim B, Schar M, Park H, Heo HY. Unsupervised learning for magnetization transfer contrast MR fingerprinting: application to CEST and nuclear Overhauser enhancement imaging. *Magn Reson Med*. 2021;85(4):2040-2054. doi:10.1002/mrm.28573
88. Perlman O, Herz K, Zaiss M, Cohen O, Rosen MS, Farrar CT. CEST MR-fingerprinting: practical considerations and insights for acquisition schedule design and improved reconstruction. *Magn Reson Med*. 2020;83(2):462-478. doi:10.1002/mrm.27937
89. Kang B, Kim B, Park H, Heo HY. Learning-based optimization of acquisition schedule for magnetization transfer contrast MR fingerprinting. *NMR Biomed*. 2021;e4662. doi:10.1002/nbm.4662
90. Pillai DR, Dittmar MS, Baldaranov D, et al. Cerebral ischemia-reperfusion injury in rats—a 3 T MRI study on biphasic blood–brain barrier opening and the dynamics of edema formation. *J Cereb Blood Flow Metab*. 2009;29(11):1846-1855. doi:10.1038/jcbfm.2009.106
91. Zaiss M, Windschuh J, Paech D, et al. Relaxation-compensated CEST-MRI of the human brain at 7T: unbiased insight into NOE and amide signal changes in human glioblastoma. *NeuroImage*. 2015;112:180-188. doi:10.1016/j.neuroimage.2015.02.040
92. Goerke S, Breitling J, Korzowski A, et al. Clinical routine acquisition protocol for 3D relaxation-compensated APT and rNOE CEST-MRI of the human brain at 3T. *Magn Reson Med*. 2021;86(1):393-404. doi:10.1002/mrm.28699
93. Xu X, Yadav NN, Zeng H, et al. Magnetization transfer contrast-suppressed imaging of amide proton transfer and relayed nuclear Overhauser enhancement chemical exchange saturation transfer effects in the human brain at 7T. *Magn Reson Med*. 2016;75(1):88-96. doi:10.1002/mrm.25990
94. Chen L, Xu X, Zeng H, et al. Separating fast and slow exchange transfer and magnetization transfer using off-resonance variable-delay multiple-pulse (VDMP) MRI. *Magn Reson Med*. 2018;80(4):1568-1576. doi:10.1002/mrm.27111
95. Kim M, Gillen J, Landman BA, Zhou J, van Zijl PC. Water saturation shift referencing (WASSR) for chemical exchange saturation transfer (CEST) experiments. *Magn Reson Med*. 2009;61(6):1441-1450. doi:10.1002/mrm.21873
96. Schuenke P, Windschuh J, Roeloffs V, Ladd ME, Bachert P, Zaiss M. Simultaneous mapping of water shift and B_1 (WASABI)—application to field-inhomogeneity correction of CEST MRI data. *Magn Reson Med*. 2017;77(2):571-580. doi:10.1002/mrm.26133
97. Tietze A, Blicher J, Mikkelsen IK, et al. Assessment of ischemic penumbra in patients with hyperacute stroke using amide proton transfer (APT) chemical exchange saturation transfer (CEST) MRI. *NMR Biomed*. 2014;27(2):163-174. doi:10.1002/nbm.3048
98. Foo LS, Larkin JR, Sutherland BA, et al. Study of common quantification methods of amide proton transfer magnetic resonance imaging for ischemic stroke detection. *Magn Reson Med*. 2021;85(4):2188-2200. doi:10.1002/mrm.28565
99. Shah S, Luby M, Poole K, et al. Screening with MRI for Accurate and Rapid Stroke Treatment: SMART. *Neurology*. 2015;84(24):2438-2444. doi:10.1212/WNL.0000000000001678

100. Sablot D, Ion I, Khlifa K, et al. Target door-to-needle time for tissue plasminogen activator treatment with magnetic resonance imaging screening can be reduced to 45 min. *Cerebrovasc Dis*. 2018;45(5/6):245-251. doi:10.1159/000489568
101. Adil MM, Luby M, Lynch JK, et al. Routine use of FLAIR-negative MRI in the treatment of unknown onset stroke. *J Stroke Cerebrovasc Dis*. 2020; 29(9):105093. doi:10.1016/j.jstrokecerebrovasdis.2020.105093
102. Majidi S, Luby M, Lynch JK, et al. MRI-based thrombolytic therapy in patients with acute ischemic stroke presenting with a low NIHSS. *Neurology*. 2019;93(16):e1507-e1513. doi:10.1212/WNL.0000000000008312
103. Hsia AW, Luby ML, Leigh R, et al. Prevalence of imaging targets in patients with minor stroke selected for IV tPA treatment using MRI: the Treatment of Minor Stroke With MRI Evaluation Study (TIMES). *Neurology*. 2021;96(9):e1301-e1311. doi:10.1212/WNL.0000000000011527
104. Zheng S, van der Bom IM, Zu Z, Lin G, Zhao Y, Gounis MJ. Chemical exchange saturation transfer effect in blood. *Magn Reson Med*. 2014;71(3): 1082-1092. doi:10.1002/mrm.24770
105. Zhang H, Wang W, Jiang S, et al. Amide proton transfer-weighted MRI detection of traumatic brain injury in rats. *J Cereb Blood Flow Metab*. 2017; 37(10):3422-3432. doi:10.1177/0271678X17690165

How to cite this article: Heo H-Y, Tee YK, Harston G, Leigh R, Chappell MA. Amide proton transfer imaging in stroke. *NMR in Biomedicine*. 2022;e4734. doi:10.1002/nbm.4734